

thus varying  $T_w$ . However, in the present tests the stagnation temperature was varied to produce a slight change in  $T_w/T_t$ . This change in the stagnation temperature level may have influenced the behavior of transition by altering the effect of other interrelated parameters, such as radiated aerodynamic noise from the tunnel sidewalls. The metal cone transition data illustrates the sometimes inconsistent behavior of transition in conventional wind tunnels.

### Conclusions

Transition Reynolds numbers were lower for the ablating cones as compared to the nonablating cone, indicating an influence of mass injection on transition. There was a strong unit Reynolds number effect on the ablating cone transition Reynolds numbers. Transition Reynolds numbers obtained on the metal cone displayed both a weak and strong effect of unit Reynolds number, depending on the tunnel stagnation temperature, and thus indicated an influence of small changes in tunnel conditions on boundary-layer transition.

### References

- Wilkins, M. E. and Tauber, M. E., "Boundary-Layer Transition on Ablating Cones at Speeds up to 7 km/sec," *AIAA Journal*, Vol. 4, No. 8, Aug. 1966, pp. 1344-1348.
- Mateer, G. G. and Larson, H. K., "Unusual Boundary-Layer Transition Results on Cones in Hypersonic Flow," AIAA Paper 68-40, New York, 1968.
- Larson, H. K. and Mateer, G. G., "Transition Measurements on Cones in Hypersonic Flow and Preliminary Observations of Surface Ablation Grooves," presented at Boundary-Layer Transition Specialists Study Group Meeting, Aerospace Corp., San Bernardino, Calif., July 11-12, 1967.
- DiCristina, V., "Three-Dimensional Laminar Boundary Layer Transition on a Sharp 8° Cone at Mach Number 10," AIAA Paper 69-12, New York, 1969.
- Chapman, D. R., Kuehn, D. M., and Larson, H. K., "Investigation of Separated Flows in Supersonic and Subsonic Streams with Emphasis on the Effect of Transition," Rept. 1356, 1958, NACA.

## Shock-Wave Shapes on Hypersonic Axisymmetric Power-Law Bodies

G. S. BEAVERS\*

University of Minnesota, Minneapolis, Minn.

IN this Note experimental observations are reported on the shock-wave shapes over axisymmetric power-law bodies, of the form  $y \sim x^{m_b}$ , situated in a hypersonic flow. These measurements were made in an attempt to verify certain aspects of asymptotic hypersonic flow theory, where the term asymptotic refers to the flowfield at large distances downstream of the nose of the body. Although the calculation of the asymptotic flowfield for power-law bodies has received considerable attention in the past few years, relatively few experimental observations appear to have been reported in the literature. Freeman, Cash, and Bedder<sup>1</sup> made observations on the shock shapes over seven axisymmetric power-law bodies for values of the exponent  $m_b$  in the range  $0 \leq m_b \leq 1$ , and concluded that the comparison between theory and experiment was far from satisfactory. Kubota<sup>2</sup> reported more complete data on the asymptotic flowfields, including shock

shapes, surface pressure distributions and shock layer pressure traverses, for three axisymmetric power-law bodies with  $m_b = \frac{1}{2}$ ,  $\frac{2}{3}$ , and  $\frac{3}{4}$ . Other data on axisymmetric shock shapes have been obtained by Peckham<sup>3</sup> and appear to be similar to those of Ref. 1. Information on the flowfields and shock shapes over plane power-law bodies has been reported by Hornung<sup>4</sup> for  $m_b = \frac{1}{2}$  and  $\frac{5}{8}$ .

It is well known that when the freestream Mach number  $M$  is sufficiently large, the hypersonic small-disturbance equations possess similar solutions for the asymptotic shock-wave shapes over power-law bodies. These solutions state that the shock-wave shapes for axisymmetric power-law bodies are given by  $y \sim x^{m_b}$ , where

$$m_b = m_s \quad \text{for} \quad \frac{1}{2} < m_b \leq 1 \quad (1a)$$

and

$$m_b = \frac{1}{2} \quad \text{for} \quad 0 \leq m_b < \frac{1}{2} \quad (1b)$$

The solutions (1a) were obtained by Lees and Kubota,<sup>5</sup> and correspond to the situation in which the asymptotic flowfield is dominated by the shape of the body. The solutions (1b) are the blast-wave analogy solutions of Lees<sup>6</sup> and Cheng and Pallone,<sup>7</sup> and are appropriate to those body shapes in which the asymptotic flowfield is dominated by the nose bluntness of the body. The solutions (1) may be used as first approximations in asymptotic solutions for the shock-wave shapes. This is discussed by Freeman,<sup>8</sup> who shows in particular that for the range  $\frac{1}{2}\gamma < m_b < \frac{1}{2}$  the first correction term to the blast wave solution is due to the perturbation introduced by the body shape. The correction to the shock shape and to the asymptotic flowfield in general for this range of  $m_b$  has been computed by Hornung.<sup>9</sup>

In this work a comprehensive study has been made of shock-wave shapes on axisymmetric power-law bodies in the range  $0 \leq m_b \leq 1$  in an attempt to verify the first-order solutions (1). Comparisons are made with the results of Freeman and co-workers, and the effects of Hornung's correction term to the first-order solution for  $m_b = 0.4$  are indicated.

The experiments were run in the Rosemount Aeronautical Laboratory 12-in.  $\times$  12-in. hypersonic wind tunnel at a freestream Mach number of 7.0. Most of the runs were made at a stagnation pressure of 115 psia and a Reynolds number of  $6 \times 10^6$ /in. Several tests were repeated at a stagnation pressure of 135 psia and a corresponding Reynolds number of about  $10^7$ /in. No evident trends in the final data with Reynolds number could be detected. Two families of power-law bodies were used, each family consisting of eight models with values of  $m_b$  of 0, 0.1, 0.25, 0.4, 0.5, 0.7, 0.85, and 1.0. The lengths of the two sets were 7 in. and 4 in., and all bodies had a maximum diameter of 2 in. Shock shapes were mea-

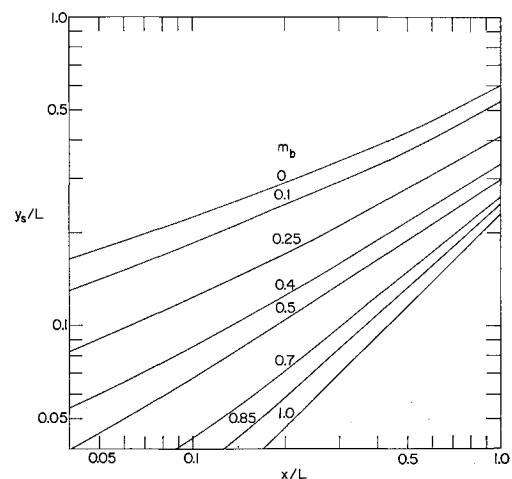


Fig. 1 Typical shock-wave shapes for 7-in. bodies ( $M = 7.0$ ).

Received May 26, 1969. This research was supported by NASA under grant NGR-24-005-063 to the Space Science Center, University of Minnesota.

\* Assistant Professor, Department of Aeronautics and Engineering Mechanics. Member AIAA.

sured directly from shadowgraphs taken on 11-in. × 14-in. x-ray plates, which provided very sharp definitions of the edges of the shocks.

Several shadowgraphs were obtained for each body, and the resultant shock shapes were plotted logarithmically as in Fig. 1, where  $L$  is the length of the body in the axial direction  $x$ . The slopes of these curves give the values of the exponent  $m_s$  directly. Unlike the results of Ref. 1, in which a considerable variation of the exponent  $m_s$  with  $x$  was found for any particular shock, all the shocks measured in the current experiments exhibited constant values for  $m_s$  after an initial variation over the front part of the body. The distance for  $m_s$  to become constant varied from a value of  $x/L$  of about 0.2 for  $m_b = 0.85$  to a value of about 0.6 for  $m_b = 0$ . The constant values of  $m_s$  are plotted against the corresponding values of  $m_b$  in Fig. 2. The top two parts of this figure show the average values of  $m_s$  for a given  $m_b$  for the 7-in. and 4-in. models, together with the ranges over which the values were obtained. As observed by Freeman and co-workers<sup>1</sup> and Peckham,<sup>3</sup> the experimentally obtained variation of  $m_s$  with  $m_b$  is a smoothed version of that predicted from similarity results, with the largest discrepancy occurring at  $m_b = 0.5$ . This is to be expected since at this value the similarity assumption is no longer valid, and the error terms as computed by Freeman<sup>8</sup> dominate the flowfield.

The present results are compared with those from Ref. 1 in the bottom part of Fig. 2, where the latter results are plotted for  $x/L = 0.5$  with the variation over the range  $0.2 < x/L < 1.0$  also shown. The variation in  $m_s$  as  $m_b$  decreases from about 0.4 to 0 appears to be much smaller for the present results than for the results of Refs. 1 and 3. This small variation in  $m_s$  is consistent with the predictions of Freeman<sup>8</sup> that the error term is of constant order in  $M^{-2}$  over the range  $0 < m_b < \frac{1}{2}\gamma$ . Two results obtained by Kubota<sup>2</sup> are also shown in Fig. 2. It has been remarked elsewhere<sup>1,8</sup> that the excellent agreement of these data with theory is probably due in part to a judicious choice of the shock slope.

Hornung<sup>4</sup> suggested a means of correlating shock shapes for bodies having the same exponent  $m_b$ . If the body shape is expressed in the form  $y/d = (x/d)^{m_b}$ , then for large  $M$  the shock shapes for all bodies having a particular  $m_b$  collapse on to a single curve in these coordinates. Such plots are shown in Fig. 3 for  $m_b = 0.1$  and 0.85, and in Fig. 4 for  $m_b = 0.25, 0.4, 0.5,$  and 0.7. For each value of  $m_b$  points from several shock waves are shown. It may be observed from Figs. 3 and 4

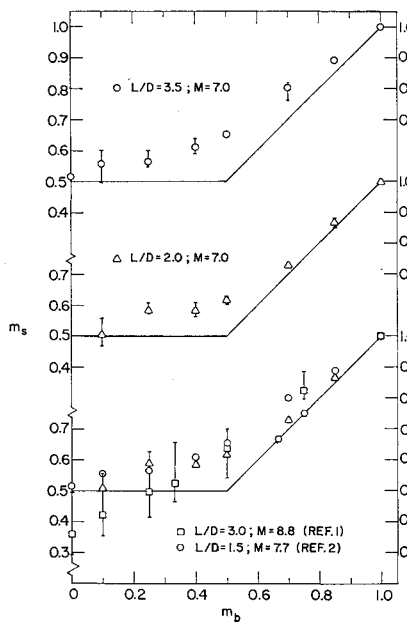


Fig. 2 Shock exponent  $m_s$  vs body exponent  $m_b$ .

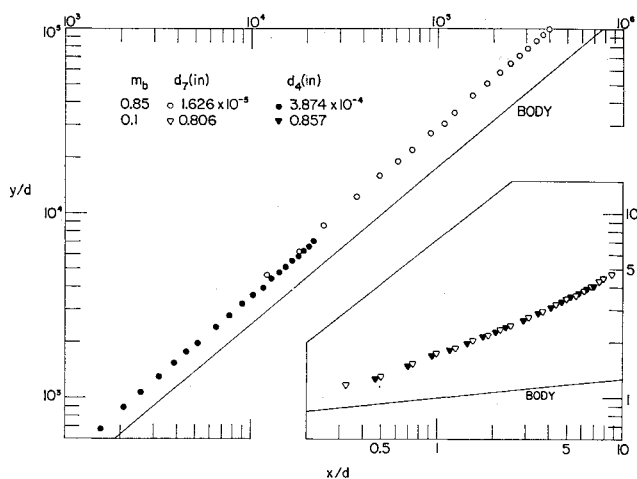


Fig. 3 Correlation of shock-wave shapes;  $m_b = 0.1$  and 0.85.

that the shocks for  $m_b = 0.1, 0.25,$  and  $0.4$  all appear to collapse very closely onto a single curve.

The aforementioned expansion procedure used by Hornung<sup>9</sup> involves a constant that requires for its evaluation a knowledge of the drag of the body in question. In order to give a qualitative indication of the effect of the second-order terms derived by Hornung a value of the constant was chosen such that the first-order solution (i.e. the blast-wave analogy solution) passed through the last point on the plot of  $y/d$  against  $x/d$  for  $m_b = 0.4$ , Fig. 4. The second-order solution was computed from Hornung's theory, and it is seen that the estimate for the deviation from the first-order theory is much too small although it does correct the first-order theory in the right direction.

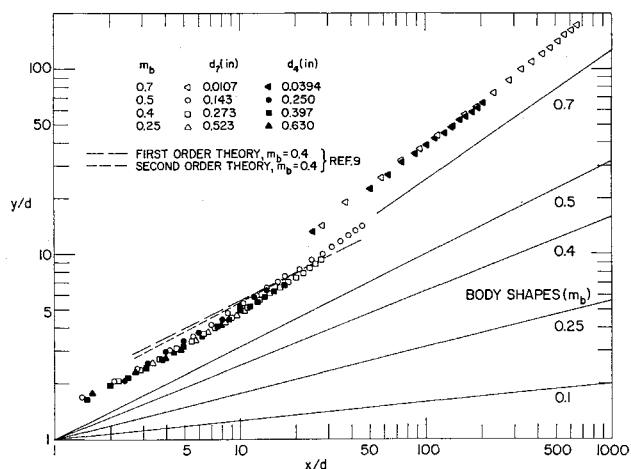


Fig. 4 Correlation of shock-wave shapes;  $m_b = 0.25, 0.4, 0.5,$  and 0.7.

References

- <sup>1</sup> Freeman, N. C., Cash, R. F., and Bedder, D., "An Experimental Investigation of Asymptotic Hypersonic Flows," *Journal of Fluid Mechanics*, Vol. 18, No. 3, March 1964, pp. 379-384.
- <sup>2</sup> Kubota, T., "Inviscid Hypersonic Flow over Blunt-Nosed Slender Bodies," Publication 417, 1957, Graduate Aeronautical Lab., California Institute of Technology.
- <sup>3</sup> Peckham, D. H., "Measurements of Pressure Distribution and Shock-Wave Shape on Power-Law Bodies at a Mach Number of 6.85," 27084, April 1965, Aeronautical Research Council.
- <sup>4</sup> Hornung, H. G., "Inviscid Hypersonic Flow over Plane Power-Law Bodies," *Journal of Fluid Mechanics*, Vol. 27, No. 2, Feb. 1967, pp. 315-336.

<sup>5</sup> Lees, L. and Kubota, T., "Inviscid Hypersonic Flow over Blunt-Nosed Slender Bodies," *Journal of the Aeronautical Sciences*, Vol. 24, March 1957, pp. 195-202.

<sup>6</sup> Lees, L., "Hypersonic Flow," *Proceedings of the 5th International Aeronautical Conference*, Institute of Aeronautical Science, 1955, pp. 241-276.

<sup>7</sup> Cheng, H. K. and Pallone, A. J., "Inviscid Leading-Edge Effect in Hypersonic Flow," *Journal of the Aeronautical Sciences*, Vol. 23, July 1956, pp. 700-702.

<sup>8</sup> Freeman, N. C., "Asymptotic Solutions in Hypersonic Flow: An Approach to Second-Order Solutions of Hypersonic Small-Disturbance Theory," *Research Frontiers in Fluid Dynamics*, edited by R. J. Seeger and G. Temple, Interscience, New York, 1965, pp. 284-307.

<sup>9</sup> Hornung, H. G., "Inviscid Hypersonic Flow over Axisymmetric Power-Law Bodies," ARL/A 288, May 1967, Australian Defense Scientific Service, Aeronautical Research Lab., Melbourne, Australia.

## Stagnation-Point Velocity Gradients for Spherical Segments in Hypersonic Flow

LARRY L. TRIMMER\*

ARO Inc., Arnold Air Force Station, Tenn.

AND

EDWARD L. CLARK†

Sandia Laboratory, Albuquerque, N. M.

### Nomenclature

- $\alpha$  = speed of sound  
 $M$  = Mach number  
 $p$  = pressure  
 $S$  = surface distance from stagnation point  
 $U$  = velocity  
 $\gamma$  = ratio of specific heats  
 $\theta$  = surface angle measured from stagnation point

### Subscripts

- $l$  = local conditions  
 $s$  = stagnation point conditions  
 $\infty$  = free-stream conditions

### Superscript

- \* = sonic conditions

### Introduction

**H**YPERSONIC convective stagnation heating of blunt bodies has been shown theoretically<sup>1</sup> to be dependent on the square root of the velocity gradient at the stagnation point. Theoretical or experimental determination of the stagnation-point velocity gradient is, therefore, required to predict the stagnation heating of a particular configuration. Considerable effort has been expended on blunt body flowfield numerical solutions; however, there is a distinct lack of reliable experimental data in this area. A particular family of blunt bodies, the spherical segment, was studied experimentally by Boison and Curtiss<sup>2</sup> at Mach numbers from 2.01 to 4.76. Additionally, Kendall<sup>3</sup> presented data for shapes that com-

Received May 23, 1969. The research presented in this paper was supported by the Arnold Engineering Development Center (AEDC), Air Force Systems Command (AFSC), U.S. Air Force, under Contract F40600-69-C-0001 with ARO Inc.

\* Group Supervisor, Aerodynamics Division, von Kármán Gas Dynamics Facility. Associate Member AIAA.

† Staff Member, Experimental Aerodynamics Division, Aerothermodynamics Projects Department; formerly Project Engineer, von Kármán Gas Dynamics Facility (VKF), ARO Inc.

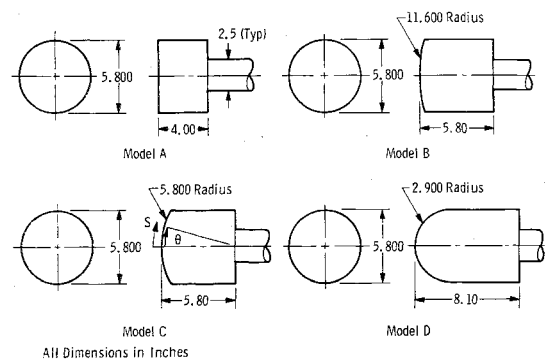


Fig. 1 Test models.

prise the extremities of the spherical segment family (i.e., the flat-nose cylinder and the hemisphere) over a similar Mach number range. It was the purpose of the present study to extend the experimental results of these references to hypersonic Mach numbers. Tests at Mach numbers 6, 8, and 10 and freestream Reynolds numbers of about  $1.0 \times 10^6$ , based on model diameter, were conducted in the von Kármán Facility's 50-in. hypersonic wind tunnels. Pressure distributions were measured on four spherical segment models (Fig. 1) ranging in bluntness from a hemisphere to a flat-nose cylinder (the flat-nose cylinder is considered to be a spherical segment with infinite nose radius). Detailed results of these tests are given in Ref. 4.

### Analysis

When a sphere is cut ahead of the natural sonic point ( $\theta \approx 42^\circ$  at hypersonic Mach numbers), the subsonic flow over the sphere is forced to adapt to the sonic condition at the corner. To provide a parameter that is compatible with the geometric and aerodynamic restrictions imposed by the spherical segment, the surface arc length  $S$  nondimensionalized by the surface length to the sonic point  $S^*$  is used as the independent variable in this analysis. The variation of the experimental pressure distributions with this parameter is presented in Fig. 2. Theoretical estimates of the pressure distribution, based on the modified Newtonian theory, are also shown in Fig. 2. The agreement between theory and experiment is very good for the hemisphere but becomes poorer as the bluntness is increased. No appreciable Mach number effects were observed for the range of test conditions ( $M_\infty = 6-10$ ) covered by the present tests. For models A, B, and C, the sonic point  $\theta^*$  was assumed to be at the shoulder giving sonic point values of 0, 14.48, and  $30.00^\circ$ , respectively. For the hemisphere,  $\theta^*$  is a function of freestream

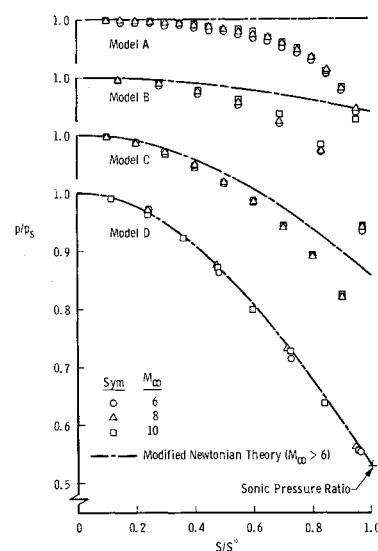


Fig. 2 Model pressure distributions.